Economic Operation of a Micro-Grid considering Demand Side Flexibility and Common ESS Availability

Ayşe Kübra Erenoğlu, İbrahim Şengör, and Ozan Erdinç
Yildiz Technical University, Turkey
{erenayse, isengor, erdinc}@yildiz.edu.tr

Akın Taşcıkaraoğlu
Mugla Sitki Kocman University Turkey
akintascikaraoglu@mu.edu.tr

João P. S. Catalão
INESC TEC and FEUP, Porto, C-MAST/UBI, Covilha, and INESC-ID/IST-UL, Lisbon, Portugal
catalao@ubi.pt

***Abstract*—The micro-grid concept has recently gained increasing attention for power system operators to increase the operational effectiveness and provide a more reliable, sustainable and economic power system. To ensure the autonomous power supply when disconnected from the bulk power system, energy storage system (ESS) options as well as demand side flexibility can be used to provide the local balance between time-varying production and consumption in a micro-grid structure. In this study, the demand side flexibility via thermostatically controllable appliances (TCAs)-based direct load control (DLC) strategies and common ESSs-based bi-directional energy flow possibility is considered for the economic operation of a micro-grid. Different case studies are conducted for validating the effectiveness of the proposed structure.**

***Index Terms*—Common energy storage system; demand side flexibility; economic operation; electric vehicle; micro-grids.**

NOMENCLATURE

The main nomenclature used throughout this study is stated in Table I-III.

TABLE I. SETS AND INDICES

b	Set of branches.
c	Set of wind turbines.
f	Set of PV farms.
h	Set of residential end-users in each residential type.
i	Set of nodes.
k	Set of residential end-user types.
l	Set of commercial end-user types.
t	Set of time periods.
Ω_i^f	Subset of substation nodes.

TABLE II. PARAMETERS

$CE_{k,h}^{EV,res}$	EV charging efficiency of type k residential end-user h.
$CE_l^{EV,com}$	EV charging efficiency of type l commercial end-user.
$COP_{k,h}$	Coefficient-of-performance for type k residential end-user h.
COP_l	Coefficient performance for type l commercial end-user.
f_b^{max}	Flow limit of branch b [kW].
N	Sufficiently large positive constant.
$P_{c,t}^{wind}$	Power production for wind turbine c in period t [kW].
$P_{f,t}^{pv}$	Power production for PV farm f in period t [kW].
$P_i^{f,max}$	Maximum power that feeder of node i can provide [kW].
$P_{k,h,t}^{res,inflex}$	Inflexible load of type k residential end-user h in period t [kW].
$P_{k,h}^{res,AC}$	Air conditioner rated power for type k residential end-user h [kW].
$P_{l,t}^{com,inflex}$	Inflexible load of type l end-user in period t [kW].
$P_l^{com,AC}$	Air conditioner rated power for type l commercial end-user [kW].
P_t^{ind}	Power consumption of industrial premise in period t [kW].
$P_t^{pv,tot}$	Total PV power production in period t [kW].
$P_t^{wind,tot}$	Total wind power production in period t [kW].
$R_{k,h}^{EV,ch,res}$	EV charging rate for type k residential end-user h [kW].
$R_l^{EV,ch,com}$	EV charging rate for type l commercial end-user [kW].
$SOE_{k,h}^{EV,ini,res}$	EV initial SOE of type k residential end-user h [kWh].
$SOE_{k,h}^{EV,max,res}$	EV maximum SOE of type k residential end-user h [kWh].
$SOE_{k,h}^{EV,min,res}$	EV minimum SOE of type k residential end-user h [kWh].
$SOE_l^{EV,ini,com}$	EV initial SOE of type l commercial end-user [kWh].
$SOE_l^{EV,max,com}$	EV maximum SOE of type l commercial end-user [kWh].
$SOE_l^{EV,min,com}$	EV minimum SOE of type l commercial end-user [kWh].
$SP_{k,h,t}^{res,AC}$	Air conditioner temperature set point for type k residential end-user h in period t [℃].
$SP_{l,t}^{com,AC}$	Air conditioner temperature set point for type l commercial end-user in period t [℃].
t_1	Starting period of the contracted DR period for residential end-users.
t_2	Ending period of the contracted DR period for residential end-users.
t_3	Starting period of the contracted DR period for commercial end-users.
t_4	Ending period of the contracted DR period for commercial end-users.
$T_{k,h,r}^a$	EV arrival time of type k residential end-user h.
$T_{k,h,r}^d$	EV departure time of type k residential end-user h.
$T_{k,h}^{res,desired}$	Desired comfort temperature level of type k residential end-user h [℃].
$T_{k,h}^{res,down}$	Maximum allowed temperature set-point decrease from the desired comfort temperature level of type k residential end-user h during DR event [℃].
$T_{k,h}^{res,up}$	Maximum allowed temperature set-point increase from the desired comfort temperature level of type k residential end-user h during DR event [℃].
$T_l^{EV,com,a}$	EV arrival time of type l commercial end-user.
$T_l^{EV,com,d}$	EV departure time of type l commercial end-user.
$T_l^{com,desired}$	Desired comfort level of type l commercial end-user [℃].
$T_l^{com,down}$	Maximum allowed temperature set-point decrease from the desired comfort temperature level of type l commercial end-user during DR event [℃].
$T_l^{com,up}$	Maximum allowed temperature set-point increase from the desired comfort temperature level of type l commercial end-user during DR event [℃].
T_t^a	Outdoor air temperature [℃].

TABLE III. VARIABLES

$F_{b,t}$	Approximate value of the square of the flow through branch b during period t [kW^2].
$f_{b,t}$	Active power flow of branch b during period t [kW].
$P_{b,t}^{loss}$	Power losses of branch b during period t [kW].
$P_{i,t}^{f,load}$	Active power provided by substation at node i during period t to cover demand [kW].
$P_{i,t}^f$	Total active power provided by substation at node i during period t [kW].
$P_{k,h,t}^{EV,ch,res}$	EV charging power of type k residential end-user h in period t [kW].
$P_{k,h,t}^{res,AC}$	Air conditioner power consumption of type k residential end-user h in period t [kW].
$P_{k,h,t}^{res}$	Consumed power of type k residential end-user h in period t [kW].
$P_{l,t}^{EV,ch,com}$	Charging power of type l commercial end-user in period t [kW].
$P_{l,t}^{com,AC}$	Air conditioner power consumption of type l commercial end-user in period t [kW].
$P_{l,t}^{com}$	Power consumption of type l commercial end-user in period t [kW].
$P_t^{com,total}$	Total power consumption of all commercial end-users in period t [kW].
$P_t^{res,total}$	Total power consumption of residential end-users in period t [kW].
$P_t^{sell,grid}$	Power injected to grid in period t [kW].
$SOE_{k,h,t}^{EV,res}$	EV SOE of type k residential end-user h in period t [kWh].
$SOE_{l,t}^{EV,com}$	EV SOE of type l commercial end-user in period t [kWh].
$S_t^{com,d}$	Deviation of the commercial end-user indoor temperature from the ideal point to down side in period t [℃].
$S_t^{com,u}$	Deviation of the commercial end-user indoor temperature from the ideal point to upper side in period t [℃].
$S_t^{res,d}$	Deviation of the residential end-user indoor temperature from the ideal point to down side in period t [℃].
$S_t^{res,u}$	Deviation of the residential end-user indoor temperature from the ideal point to upper side in period t [℃].
$T_{k,h,t}^{r,res}$	Room temperature of type k residential end-user h [℃].
$T_{l,t}^{r,com}$	Room temperature of type l commercial end-user in period t [℃].
$u_{k,h,t}^{EV,res}$	Binary variable. 1 if EV is charging in period t; else 0.
$u_{k,h,t}^{res,AC}$	Binary variable. 1 if the air conditioner of type k residential end-user h is operating in period t; else 0.
$u_{l,t}^{EV,com}$	Binary variable. 1 if EV is charging in period t; else 0.
$u_{l,t}^{com,AC}$	Binary variable. 1 if the air conditioner of type l commercial end-user is operating in period t; else 0.
u_t^{grid}	Binary variable. 1 if micro-grid is drawing power from the main grid in period t; else 0.

978-1-5386-4505-5/18/$31.00 ©2018 IEEE

INTRODUCTION

A. Motivation and Background

In modern power grid, micro-grids (MGs) as small-scale energy systems consisting of local loads, distributed generation (DG) units and energy storage systems (ESSs) are developing fast and have gained increasingly importance worldwide [1]. MGs can be operated in two different modes, namely, islanded and grid-connected (non-isolated) modes. In grid-connected mode, there is an opportunity to exchange power with the main grid through point of common coupling (PCC). On the other hand, MG can be disconnected from the main grid easily, e.g. in case of upstream disturbances, and should continue to supply power to the local end-users in islanded mode. Due to increasing environmental concerns and climate change, there is also a strong trend towards integrating renewable energy sources (RESs) based production units such as solar, wind, hydro and biomass into MGs [2]. However, penetration of RESs that provide highly volatile and intermittent power output may cause significant challenge in MG operation. Besides, apart from the fluctuation in generation side, there is also uncertainty in market prices and demand with new types of electric loads such as electric vehicles (EVs), and these issues raise concerns about providing supply-demand balance and maintaining the voltage/frequency stability in MGs [3].

In fact, there are many ways to deal with the aforementioned problems such as using conventional and controllable generating systems, ESSs and lastly but most promising approach by using demand side flexibility via demand response (DR) programs owing to the smart grid concept. DR programs can be classified into two groups which are indirect load control (ILC) and direct load control (DLC) approaches. DLC approach is generally utilized more for immediate actions compared to ILC approaches and the most common DLC-oriented appliances in residential end-user premises are electric water heaters (EWHs), air conditioners (ACs), and refrigerators due to their rapid response in case of instantaneous variations in switching conditions. Besides, these flexible loads are also called Thermostatically Controlled Loads (TCLs) [4].

According to above mentioned information, it is clearly seen that today's MGs consist of several types of generation sources such as dispatchable and non-dispachable generating units, ESS units, different type of loads and also prosumers (end-users also with on-site production facilities). Here, an energy management system (EMS) is strongly needed to effectively and efficiently schedule the operational issues of new generation MGs with such stochastic characteristics.

B. Relevant Background

In recent years, there has been an increasing amount of literature on EMS strategies by taking into account different combined structures for providing optimal operation of MGs.

Kanchev et al. [5] proposed a dynamic programming based multi-objective EMS structure compromising the minimization of operational costs and CO_2 emissions for residential MGs including photovoltaic (PV)-based production units and batteries. The study in [6] proposed an optimization algorithm providing optimal dispatch of ESS and RESs by utilizing them as much as possible for decreasing fuel-based programmable units ratio in MGs. Abedini et al. [7] developed an optimization strategy for providing economic operation and optimal design of MGs containing PV, wind, diesel generator hybrid energy system and stationary batteries. Gazijahani et al. [8] suggested a day ahead power scheduling model specifically focusing on stochastic nature of RESs and unpredictable/uncertain electricity demand for MGs by applying grey wolf optimization algorithm in a scenario-based approach. The above mentioned references investigated the impact of DR and EVs in the proposed EMS models and accordingly benefits of these combined systems in terms of optimal operation of MGs were not indicated. Most of the researches available in the literature for incorporating DR mechanisms into EMS offer ancillary services to improve system efficiency, sustainability and to facilitate large scale RES integration in MGs. In this manner, Solanki et al. [9] presented a model predictive control based MG EMS approach in order to reduce deviations in the forecast of the RES generation and variable electricity demand. Also, a neural network based model has been suggested in [9] for determining controllable loads' demand profile and utilizing their energy reduction capability by integrating this algorithm into the EMS structure. Lopez et al. [10] proposed a decentralized optimal management strategy for MGs including RES units, dispatchable generation systems and demand flexibility via price-based DR programs so as to schedule demand curve and operate MGs economically and efficiently. Pourmousavi et al. [11] presented a power management algorithm for providing economic and safe operation of residential MGs assuming that the stationary batteries and DR source of EWH were used for mitigating generation-consumption deviations in a MG structure where energy production is provided by PV systems and diesel generation units. However, different type of controllable appliances that have a crucial role in demand shape in residential MGs such as ACs have not been investigated and also, different types of end-users (residential, industrial, and commercial) were not considered in [11]. Zhang et al. [12] proposed a robust two-stage MG coordination strategy, which enabled to apply price based DR in the first stage based on dynamic day ahead prices and in the second stage, presented strategy could control/coordinate dispatchable generation systems to address the mismatches. However, the DLC based DR strategies as well as the interactions with different end-user types were not taken into consideration in [12].

The aforementioned studies and many other studies that could not all be referred here have contributed to a growing interest in improving MGs performance. However, some of the mentioned papers neglected the demand side flexibility in MG operation while other did not take either RES or ESS availability, and interactions with different end-user types providing different challenges and/or opportunities for MG operation.

C. Contributions

In this study, an EMS is proposed for the operation of an MG consisting of non-dispatchable resources, various type of end-users (residential, commercial, industrial), controllable and non-controllable appliances enabling DR applications, ESSs and EVs. Herein, the mathematical formulation of the system structure is based-on Mixed-Integer Linear Programming (MILP) frame with the objective of minimizing total energy losses in MGs.

The major contributions of this study can be summarized as follows:

- Incorporating different type of RESs (Wind, PV) is taken into account with the dynamic component of ESS charge/discharge strategies and also, popular new load types by EVs in order to make realistic assumptions and minimize total losses in the branches.
- DR programs are integrated in the proposed EMS strategy for utilizing thermal storage capabilities of the TCLs such as ACs by taking into account in various types of end-users such as residential, industrial and commercial in DLC approach.

D. Organization of the Paper

The remainder of the paper is organized as follows: Section II describes the proposed MG structure, its components and the mathematical model of the generation units, storage systems and controllable appliances for optimal operation of MGs. Section III carries out numerical simulations of the presented optimization problem with different case studies and afterwards, their corresponding results are demonstrated. Finally, Section VI highlights the significant conclusions, discussions and future work.

PROBLEM FORMULATION

E. Overview of the Proposed Structure

The proposed MG scheme which enables bidirectional power flow with main grid is depicted in Fig. 1.

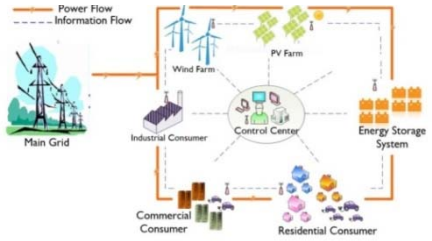

Figure 1. Proposed smart micro-grid structure

The power demand of MG is procured by main grid or/and distributed renewable and conventional locally energy supply units. Similarly, excess energy can be sold back to the main grid and/or stored in common storage systems by taking into account optimal MG operation. Multiple houses, multiple commercial end-users and industrial end-user are considered in this framework.

F. Mathematical Formulation

A comprehensive mathematical formulation of EMS based on MILP is presented in this subsection considering optimal power flow and operational constraints of the system.

B.1. Objective Function

The objective function expressed by Eq. (1) aims to minimize total losses in MG.

$$Minimize\ Losses = \sum_{t}\sum_{b} P_{b,t}^{loss} \quad \forall b \in B, t \in T \tag{1}$$

B.2. Power Balance, Branch Flow Limits, Substation Limits

$$\begin{aligned} P_t^{pv,tot} + P_t^{wind,tot} + P_t^{ESS,dis,tot} + P_{i,t}^{f,load} \\ + \sum_{b\in B:i\in\Omega_b^j} f_{b,t} - \sum_{b\in B:i\in\Omega_b^i} f_{b,t} \\ = P_t^{res,total} + P_t^{com,total} + P_t^{ind} \\ + P_t^{ESS,ch,tot} \quad \forall \mathrm{i} \in \mathrm{I}, \forall \mathrm{t} \in \mathrm{T} \end{aligned} \tag{2}$$

$$-f_b^{max} \le f_{b,t} \le f_b^{max} \quad \forall b \in B, t \in T \tag{3}$$

$$\begin{aligned} P_{i,t}^f = P_{i,t}^{f,load} + \textstyle\sum_{b\in B} P_{b,t}^{loss} + P_t^{sell,grid} \quad \forall i \in \\ \Omega_i^f, \forall \mathrm{t} \in \mathrm{T} \end{aligned} \tag{4}$$

$$P_{i,t}^f \le N \times u_t^{grid} \tag{5}$$

$$P_t^{sell,grid} \le N \times (1 - u_t^{grid}) \tag{6}$$

$$0 \le P_{i,t}^f \le P_i^{f,max} \quad \forall i \in \Omega_i^f, \forall \mathrm{t} \in \mathrm{T} \tag{7}$$

Equation (2) states the power balance in MG comprising total produced power by DG ($P_t^{pv,tot}, P_t^{wind,tot}$), the total ESS charging power ($P_t^{ESS,ch,tot}$) and actual power provided by ESS discharging ($P_t^{ESS,dis,tot}$). Additionally, total residential consumption ($P_t^{res,total}$) consisting of inflexible load, flexible load and EV charging power ($P_{k,h,t}^{res,inflex}, P_{k,h,t}^{res,AC}, P_{k,h,t}^{EV,ch,res}$), commercial users' total consumption ($P_t^{com,total}$) similarly consisting of inflexible load, flexible load and EV charging power ($P_{l,t}^{com,inflex}, P_{l,t}^{com,AC}, P_{l,t}^{EV,ch,com}$) are considered. Also, inflexible industrial load (P_t^{ind}) is considered and herein, generated power for covering demand by substation generator, the power which enters the node and is sent from i reference bus to load busses are added to the power balance equation and represented as $P_{i,t}^{f,load}$, $\sum_{b\in B:i\in\Omega_b^j} f_{b,t}$, $\sum_{b\in B:i\in\Omega_b^i} f_{b,t}$, respectively. Branch flow limit is expressed in inequality (3) and this power can be negative or positive according to optimal solution of the problem. Equation (4) is valid just for substation node and generated power ($P_{i,t}^f$) should meet the load demand of nodes ($P_{i,t}^{f,load}$) and losses of branches ($P_{b,t}^{loss}$). Inequalities (5) and (6) are constraints of determining power exchange between grid and MG. It should be noted that these logic rules prevent to sell and buy energy from the grid at the same time. N is chosen as a sufficiently large positive constant in this study, but it can also be determined as a power system asset power limitation. Finally, inequality (7) expresses the constraint of substation node's generator power limits. Here, linearization of the energy loss which is a second-order function of power flow in the lines is realized by using one of the most common techniques of Special Order Sets of Type 2 (SOS2) as explained in [13]

B.4. DG Production

$$P_t^{pv,tot} = \sum_{f} P_{f,t}^{pv} \tag{12}$$

$$P_t^{wind,tot} = \sum_{c} P_{c,t}^{wind} \tag{13}$$

Equation (12) denotes the total power provided by the PV farms ($P_t^{pv,tot}$), and similarly Eq. (13) expresses the wind turbines' power production ($P_t^{wind,tot}$), respectively.

B.5. Residential Model

$$P_t^{res,total} = \sum_{k}\sum_{h} P_{k,h,t}^{res} \tag{14}$$

$$P_{k,h,t}^{res} = P_{k,h,t}^{res,inflex} + P_{k,h,t}^{res,AC} + P_{k,h,t}^{EV,ch,res} \tag{15}$$

The total residential consumption ($P_t^{res,total}$) is shown in Eq. (14) and its components consisting of inflexible load, flexible load and EV charging power ($P_{k,h,t}^{res,inflex}, P_{k,h,t}^{res,AC}, P_{k,h,t}^{EV,ch,res}$) is denoted by Eq. (15).

B.5.1. Residential AC Model

$$\begin{aligned} T_{k,h,t}^{r,res} = \left(1 - \frac{\Delta t}{1000 \cdot M_a^{res} \cdot c_a \cdot R_{k,h}^{eq}}\right) \cdot T_{k,h,t-1}^{r,res} + \\ \frac{\Delta t}{1000 \cdot M_a^{res} \cdot c_a \cdot R_{k,h}^{eq}} \cdot T_{t-1}^{a} - \\ u_{k,h,t-1}^{res,AC} \frac{COP_{k,h} \cdot P_{k,h}^{res,AC} \cdot \Delta t}{0.000277 \cdot M_a^{res} \cdot c_a} \quad \forall t > 1 \end{aligned} \tag{16}$$

$$\begin{aligned} SP_{k,h,t}^{res,AC} - S_t^{res,d} \le T_{k,h,t}^{r,res} \\ \le SP_{k,h,t}^{res,AC} + S_t^{res,u} \quad \forall \mathrm{t}: \mathrm{SP}_{\mathrm{k,h,t}}^{\mathrm{res,AC}} \\ \neq \mathrm{NaN} \end{aligned} \tag{17}$$

$$P_{k,h,t}^{res,AC} = P_{k,h}^{res,AC} \cdot u_{k,h,t}^{res,AC} \tag{18}$$

$$\begin{aligned} T_{k,h}^{res,desired} - T_{k,h}^{res,down} \le T_{k,h,t}^{r,res} \\ \le T_{k,h}^{res,desired} + T_{k,h}^{res,up} \quad \forall t \\ \in [t_1, t_2] \end{aligned} \tag{19}$$

AC is one of the most important flexible loads and can be operated in the time when surplus of energy produced from renewables and likewise, can be switched off during shortages. The constraints written for the indoor temperature limits and thermostat set-point control mechanism (TSCM) method applied to AC operation are given in (16)-(19). Here it should be noted that equivalent thermal resistances of the house and inside mass of air are considered as in [4].

B.5.2. Residential EV Model

$$\begin{aligned} 0 \le P_{k,h,t}^{EV,ch,res} \le R_{k,h}^{EV,ch,res} \cdot u_{k,h,t}^{EV,res} \quad \forall t \\ \in [T_{k,h,r}^{a}, T_{k,h,r}^{d}] \end{aligned} \tag{20}$$

$$\begin{aligned} SOE_{k,h,t}^{EV,res} = SOE_{k,h}^{EV,ini,res} + CE_{k,h}^{EV,res} \\ \cdot P_{k,h,t}^{EV,ch,res} \cdot \Delta t \quad if\ t = T_{k,h,r}^{a} \end{aligned} \tag{21}$$

$$\begin{aligned} SOE_{k,h,t}^{EV,res} = SOE_{k,h,t-1}^{EV,res} + CE_{k,h}^{EV,res} \cdot P_{k,h,t}^{EV,ch,res} \\ \cdot \Delta t \quad \forall t \in (T_{k,h,r}^{a}, T_{k,h,r}^{d}] \end{aligned} \tag{22}$$

$$\begin{aligned} SOE_{k,h}^{EV,min,res} \le SOE_{k,h,t}^{EV,res} \\ \le SOE_{k,h}^{EV,max,res} \quad \forall t \\ \in [T_{k,h,r}^{a}, T_{k,h,r}^{d}] \end{aligned} \tag{23}$$

$$SOE_{k,h,t}^{EV,res} = SOE_{k,h}^{EV,max,res}, t = T_{k,h,r}^{d} \tag{24}$$

EV charging model is formulated in Eqs. (20)-(24) for each residential end-user. Constraint (20) denotes charging limits of EV. The State-of-Energy (SOE) of EV is described in Eqs. (21) and (22) considering arrival and departure times and also, battery's specifications. Inequality (23) is defined for determining bound of SOE in order to prevent deep-discharging which is harmful battery cycle life. In Eq. (24), it is to be noted that EVs should be fully charged depending on the departure time of occupants.

B.6. Commercial Model

$$P_t^{com,total} = \sum_l P_{l,t}^{com} \quad (25)$$

$$P_{l,t}^{com} = P_{l,t}^{com,inflex} + P_{l,t}^{com,AC} + P_{l,t}^{EV,ch,com} \quad (26)$$

Total commercial end-user's consumption ($P_t^{com,total}$) is shown in Equation (25) and (26) consisting of inflexible load, flexible load and EV charging power ($P_{l,t}^{com,inflex}, P_{l,t}^{com,AC}, P_{l,t}^{EV,ch,com}$). Commercial AC and EV model can be simply modified using residential AC and EV model.

B.7. ESS Model

The operation of the ESS for MG is represented by appropriately modifying the relevant equations given in [14].

TEST AND RESULTS

G. Input Data

The MILP-based mathematical formulation has been implemented in GAMS environment and solved with using CPLEX solver in order to provide an EMS structure optimal MG operation aiming at minimizing total losses by considering power flow. The optimization interval is selected as 5 minutes (0.0833h). A five node system is derived from [13] for analyzing the developed algorithm effects which have distributed energy production units, common ESS and various end-users as depicted in Fig. 2. The commercial end-user and two PV farms (70kW and 100kW) are assumed to be connected from node 2, common ESS (with a capacity, charging/discharging rate and efficiency of 350kWh, 100kW and 0.95, respectively) is connected at node 3, two wind turbines (200kW and 300kW) and industrial end-user have link with node 4 and lastly, residential end-users are supposed to be connected from node 5. The branches' maximum capacity is determined as 3MW, active power loss coefficients are 0.001 and 0.0003 MW^{-1} [13].

There are 3 types of end-users which are residential, commercial and industrial and each end-user may have EVs and flexible appliances. The residential end-users may be divided into three categories that affect arrival & departure time of EVs and controllable appliances' scheduling period. The inflexible load of each type of residential is shown in Fig. 3. The commercial users are assumed as office buildings and enable to utilize energy reduction capability of AC without comfort loss. There are two PV farms and two wind turbines which have different energy production levels and their power outputs depend on weather conditions. The PV and wind power production curves based on real data taken from NREL are shown in Fig. 4 and Fig. 5 [15].

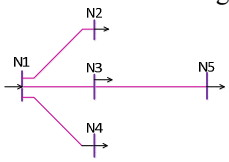

Figure 2. The 5-node distribution system

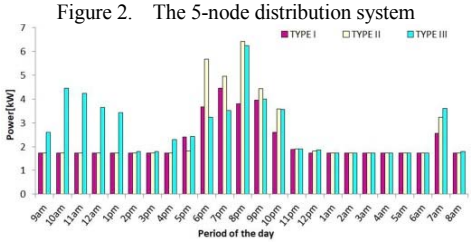

Figure 3. Daily inflexible load of different residential end-user types

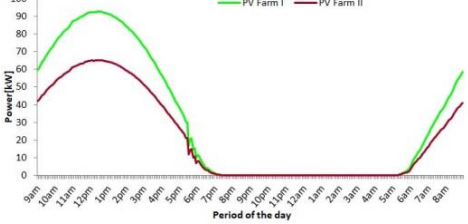

Figure 4. PV farms daily power production curve

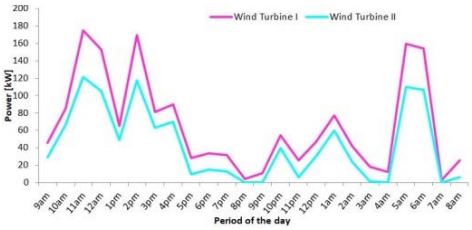

Figure 5. Wind turbines daily power production curve

TABLE IV. THE SPECIFICATIONS OF THE COMMON STORAGE SYSTEMS

	Electric Vehicle			
	Staff Service		Residential Cars	
Model	Ford Transit Jumbo	Chevy Volt	Volkswagen E-Golf	BMW i3
Battery Capacity[kWh]	51.2	16	24	22
Max Charging/ Discharging Rate [kW]	90	3.3	7.2	6.6
Charging/ Discharging Efficiency [%]	95	95	95	95
Initial SOC [%]	30	40	40	40
Minimum SOC [%]	20	20	20	20

TABLE V. TEMPERATURE-BASED PARAMETERS OF THE HOUSEHOLDS.

Parameter	Value	Units	Parameter	Value	Units
$T^{res,desired}$	20	℃	$S^{res,up}$	1	℃
$T^{res,up}$	4	℃	$S^{res,down}$	1	℃
$T^{res,down}$	3	℃			

TABLE VI. STRUCTURAL PARAMETERS OF COMMERCIAL END-USERS.

Parameter	Value	Units	Parameter	Value	Units
Office length	51.3	m	Area of windows	1.615	m^2
Office width	16	m	Wall thermal coefficient	359.57	$\frac{J}{h \cdot m \cdot ℃}$
Office height	3.6	m	Window thermal coefficient	2808	$\frac{J}{h \cdot m \cdot ℃}$
Roof angle	30	°	Thickness of windows	0.1	m
Number of windows	15	-	Thickness of walls	0.2	m

Different types of suitable EVs for residential end-users and staff service for commercial end-users are chosen [14]-[16]. End-users (e.g. type k residential end-user h) may have Chevy Volt, Volkswagen E-Golf or BMW i3, and for the commercial end-users there is one option and their arrival &departure times depend on end-users types. The specifications of the RESs, ESSs, EVs used in this study are presented in Table IV.

Residential and commercial end-user's flexible loads of ACs are utilized by their energy reduction capability in DR programs through TSCM and DCCM methods. In DCCM, AC is switched on/off directly by the LSE considering operational, comfort constraints and objective function. On the other hand, AC's thermostat set point is controlled for every kind of end-users at different time periods between 25 ℃ and 26 ℃ according to given data in Table V. All residential households and commercial buildings are chosen identical and same structural parameters for simplicity as shown in Tables VI for commercial end-users and the relevant data given in [4] for residential end-users.

Normally, air density and its thermal capacity are related to its thermodynamic properties (temperature, pressure, etc.). In this study, mentioned parameters are considered as constant and standard values are used as given in [4]. AC rated powers are determined as 2 kW for residential inhabitants, 10 kW for commercial users and the coefficient-of-performance (COP) is assumed to be 2 for every AC.

H. Simulation Results and Discussion

The presented simulation is performed in order to analyze the performance of the proposed EMS for a grid-connected MG in 5-nodes sample distribution system structure.

In this study, 7 case studies have been conducted as follows:

- **Case-1:** no flexible loads are available.
- **Case-2:** EVs are used as controllable load for both residential and commercial end-users.
- **Case-3:** Commercial end-users' EVs are charged with fast charging power.
- **Case-4:** Besides EVs, ACs are used as flexible load for just residential end-users.
- **Case-5:** Commercial end-users' EVs are charged with fast charging power.
- **Case-6:** ACs are controlled both residential and commercial end-users.
- **Case-7:** Commercial end-users' EVs are charged with fast charging power.

Fig. 6 depicts the substation node power & energy balance by showing the generated energy from slack bus, sold energy to grid, lost energy in the branches and power flow between node 1 and the other nodes. Firstly, generated energy has increased and reached the maximum value at 9am due to high level of power needs of industrial premise and commercial end-users. At this time period, PV does not generate sufficient power for covering commercial demand and similarly wind power production is at low levels. Thus, this issue results in an increase of power flow from the grid to nodes. Additionally, this increased power flow affects losses directly according to the loss function. After 6pm, the demanded power of the industrial and commercial premises decrease due to closure of these facilities and the demand of the remaining fixed loads such as interior & exterior lightning, electronic equipment loads are at about 10 kW. Also, the power production of the wind turbines increases due to higher wind speeds. Therefore, excess amount of power is sold to the main grid at 10pm, 1am, 5am, and 6am as depicted in Fig. 6.

Fig. 7 depicts the power balance at node 2 for Case-7 which commercial end-users' EVs are charged by fast-charging facilities. The power output of PV farms reaches the maximum value between 12am to 1pm. For the sake of simplicity and clarity, EVs of the same specifications are preferred for the commercial users and different charging power is used in order to investigate its effect on the system. The EV charging is performed from 12am to 2.55pm when within these periods both PV output power is continuously increasing and at the same time inflexible load of commercial users is not at highest value as shown in Fig. 7. Although, the EVs are connected to this node during 9am to 6pm, they are charged only at the mentioned periods. Therefore, it is to be noted that the charging period of commercial EV is strongly related to supply and demand power at node 2.

When the maximum charging power is determined as 12.8 kW (normal charging), the EVs are still charging during 12am to 2.55pm and they should be charged together as depicted in Fig. 8. However, when the fast charging option is activated, EVs can be charged at different time periods with higher power, especially when the period of utilized PV is very high.

DCCM DR program is implemented for scheduling commercial ACs working period during the 12am to 4pm. It is clearly shown that ACs are operated at the time when PV output increases and inflexible load decreases time interval likewise the EVs charging period. Consequently, power flow through node 2 to main grid is decreased by implementing the developed algorithm by adjusting flexible loads profiles. As a result, power losses in the branches are decreased as happened in the same event at 8am.

The existence of a common ESS provides operational flexibility via determining charging/discharging periods by developed algorithm in MG. It is evidently seen that this storage system is continuously discharging during the day instead of the charging for reducing power flow through grid to node 3 with the aim of decreasing losses considering objective function as depicted in Fig. 9.

Common storage system discharging power directly depends on residential end-users' EV charging power, inflexible loads and AC's demand. ESS is used as an energy source with high discharging power in order to cover increased residential load during especially 6pm to 10pm as shown in Fig. 9.

In order to provide optimal EMS, the ESS is operated in high discharging power when the time bus 5 power demand increases. Since the storage system minimum SOE level is determined to be 50 kWh, it is discharged with lower power in other time periods for improving system performance and minimizing total losses instead of instantaneous losses.

Fig. 10 shows the power balance at node 4 consisting of wind power production, industrial end-user demand and the power flow through grid to bus or bus to grid. Industrial premise is operated between 8am to 5.55pm and power consumption is very high.

In this optimization problem, the charging power and charging period of the EVs are determined taking into account the loss function. The differentiation of the residential end-user types has an impact on the arrival and departure times of EVs. It is clearly seen that, EVs are charged at three different time intervals which are 3.30pm-5.40pm, 10.45pm-6.55am and 7.35am-8.30am considering total inflexible load of end-users. On the other hand, EVs have been avoided to be charged as much as possible when inflexible demand increases and energy shortages may occur during peak hours at 6pm-10pm. However, after these mentioned time intervals EVs should be charged sequentially due to constraint of fully charged EV before departure time.

To investigate the changing AC's load curve effect in MG operation, it is allowed to be controlled by LSE during 12am-4pm which desired room temperature is supposed to be 20℃, up/down variations are determined as 4℃ and 3℃ respectively.

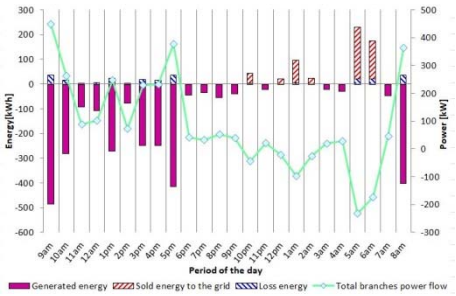

Figure 6. Case 7 node 1 power-energy balance

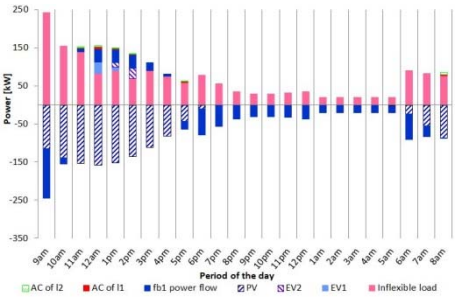

Figure 7. Case 7 node 2 power balance

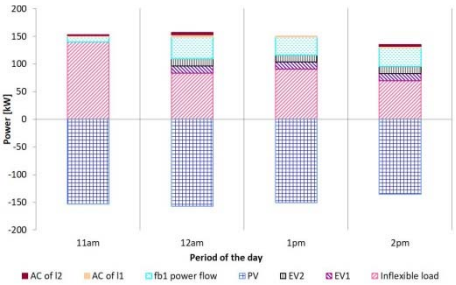

Figure 8. Case 6 node 2 power balance

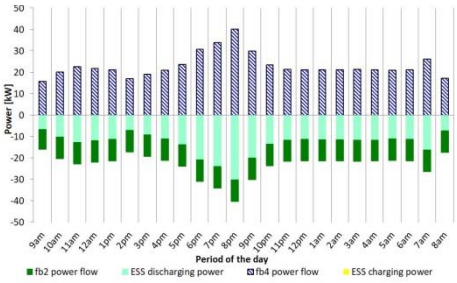

Figure 9. Case 7 node 3 power balance

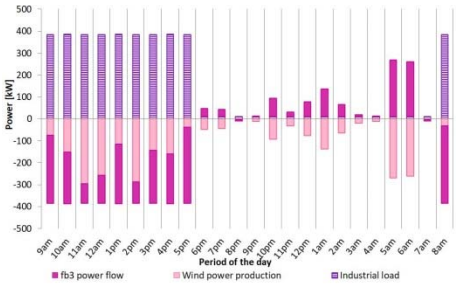

Figure 10. Case 7 node 4 power balance

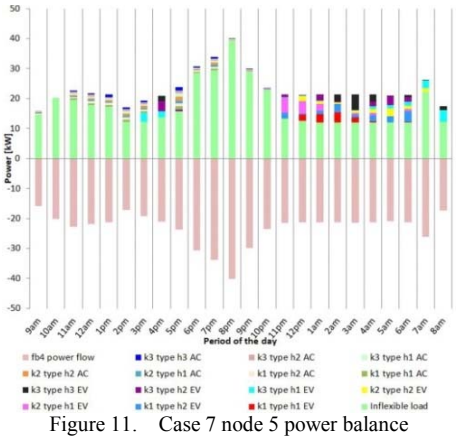

Figure 11. Case 7 node 5 power balance

TABLE VII. THE AMOUNT OF LOSS ENERGY IN THE BRANCHES FOR DIFFERENT CASE STUDIES

Case	Loss Energy	Unit	Case	Loss Energy	Unit
Case1	3094.084	kWh	**Case5**	3089.510	kWh
Case2	3081.271	kWh	**Case6**	3084.575	kWh
Case3	3080.165	kWh	**Case7**	3084.199	kWh
Case4	3090.613	kWh			

Normally, ambient temperature is prone to increase when ACs are switched off due to summer time air temperature. However, room temperature should be decreased below 24℃ before 12am considering comfort loss. Therefore, ACs are operated in during 9am-10am in order to decrease indoor temperature when fixed load is not high as shown in Fig. 11. They are switched on sequentially for the purpose of not increasing energy losses in the branches.

AC's operational period can be determined by TSCM method based on the set-point temperature which time intervals depends on residential end-user type. For example, it is assumed to be 24℃ during 11.20am-11.55am and 5.30pm-10.10pm for k_3 type h_1, h_2, h_3 end-users. At the mentioned time intervals, room temperature can vary between 23℃ and 25℃ and should not exceeded these constraints. Hence, ACs are operated in this periods.

As a consequence, it is to be noted that ACs play important role and provide flexibility to the system by DR programs in MG. When they are connected to the node which has distributed energy source, ACs are switched on with using excess available energy in order to prevent power flow from bus to the grid. On the other hand, if the power drawn from the utility is excessive and the DG production is not at the desired level, the ACs are turned off for reducing losses exactly. At beginning of the optimization (9am), the low amount of power produced by wind turbines which depends on wind speed leads to an increase amount of power flowing through grid to node 4 for meeting demand. The similar event happens at 5pm and 8am, also. On the contrary, wind power generation exceeds the industrial demand at 10pm-2pm and this time, available energy sold to the grid (but unnecessary power flow) makes losses higher. This situation happens at 5pm and 6pm, also. Hence, it is to be noted that planning of DG systems is really important in MG operation and their output power should be determined according to the objective function. The overall results are herein also summarized in Table VII.

CONCLUSION

In this study, as the main contribution to the literature on operation of the grid-connected MGs which generate energy from distributed local RESs such as PV farm and wind turbine, on the demand-side residential, commercial and industrial loads are considered with having EVs and flexible appliances, and ESS was provided in this structure for mitigating energy fluctuations. This paper presented a MILP framework-based optimization problem by formulating all aforementioned units and system in order to provide optimal EMS with the aim of minimizing total losses in the branches. Available energy could be sold to the grid or bought from the grid considering the objective function. As a result, it can be stated that ESS charging/discharging power and periods, AC's operational periods, EV charging strategies, and branches power flows cannot be evaluated independently in MG operation. All of the mentioned units have different characteristics and needs, but the MG can be operated optimally with developing optimal planning and scheduling program while satisfying constraints without significant comfort losses. In a future work, the stochastic nature of the generation units, uncertainty of arrival-departure time and state-of-energy (SOE) of the EVs and ESS's initial SOEs will be taken into account.

ACKNOWLEDGMENT

This work was mainly supported by The Scientific and Technological Research Council of Turkey (TUBITAK) under Project Grant Numbers 116E115 and 117E527. J.P.S. Catalão also acknowledges the support by FEDER funds through COMPETE 2020 and by Portuguese funds through FCT, under Projects SAICT-PAC/0004/2015 - POCI-01-0145-FEDER-016434, POCI-01-0145-FEDER-006961, UID/EEA/50014/2013, UID/CEC/50021/2013, UID/EMS/00151/2013, and 02/SAICT/2017 - POCI-01-0145-FEDER-029803, and also funding from the EU 7th Framework Programme FP7/2007-2013 under GA no. 309048.

REFERENCES

[1] A. T. Eseye, D. Zheng, H. Li, and J. Zhang, "Grid-Price dependent optimal energy storage management strategy for grid-connected industrial microgrids," *IEEE Green Technol. Conf.*, pp. 124–131, 2017.
[2] O. Egbue, D. Naidu, and P. Peterson, "The role of microgrids in enhancing macrogrid resilience," *2016 Int. Conf. Smart Grid Clean Energy Technol. ICSGCE 2016*, pp. 125–129.
[3] A. A. Zaidi, F. Kupzog, T. Zia, and P. Palensky, "Load recognition for automated demand response in microgrids," *IECON in Proc. 2016 Industrial Electron. Conf.*, pp. 2442–2447.
[4] O. Erdinc, A. Tascikaraoglu, Y. Eren, N. G. Paterakis, and J. P. S. Catalao, "End-user comfort oriented day-ahead planning for responsive residential HVAC demand aggregation considering weather forecasts", *IEEE Trans. on Smart Grid,* vol. 8, pp. 362-372, Jan. 2017.
[5] H. Kanchev, F. Colas, V. Lazarov, and B. Francois, "Emission reduction and economical optimization of an urban microgrid operation including dispatched PV-based active generators," *IEEE Trans. on Sustainable Energy*, vol. 5, pp. 1397–1405, October. 2014.
[6] S. Conti, R. Nicolosi, S. A. Rizzo, and H. H. Zeineldin, "Optimal dispatching of distributed generators and storage systems for MV islanded microgrids," *IEEE Trans. on Power Delivery,* vol. 27, pp. 1243–1251, July. 2012.
[7] M. Abedini, M. H. Moradi, and S. M. Hosseinian, "Optimal management of microgrids including renewable energy sources using GPSO-GM algorithm," *Renewable Energy,* vol. 90, pp. 430–439, 2016.
[8] F. S. Gazijahani, A. A. Abadi, H. Hosseinzadeh, and J. Salehi, "Optimal day-ahead power scheduling of microgrids considering demand and generation uncertainties," *2017 Iranian Conf. on Electrical Engineering.*, pp. 943–948.
[9] B. V. Solanki, A. Raghurajan, K. Bhattacharya, and C. A. Canizares, "Including smart loads for optimal demand response in integrated energy management systems for isolated microgrids," *IEEE Trans. on Smart Grid*, vol. 8, pp. 1739–1748, July. 2017.
[10] M. A. López, S. Martín, J. A. Aguado, and S. De La Torre, "Optimal microgrid operation with electric vehicles," *2011 IEEE PES Innovation Smart Grid Technology Conf. Europe.*, pp. 1–8.
[11] S. A. Pourmousavi, M. H. Nehrir, and R. K. Sharma, "Multi-Timescale power management for islanded microgrids including storage and demand response," *IEEE Trans. on Smart Grid*, vol. 6, pp. 1185–1195, May. 2015.
[12] C. Zhang, Y. Xu, Z. Y. Dong, and K. P. Wong, "Robust coordination of distributed generation and price-based demand response in microgrids," *IEEE Trans. on Smart Grid.*, in press.
[13] N. G. Paterakis, S. F. Santos, J. P. S. Catalão, O. Erdinc, and A. G. Bakirtzis, "Coordination of smart-household activities for the efficient operation of intelligent distribution systems," *2015 IEEE PES Innovation Smart Grid Technology Conf. Europe.,* pp. 1-6.
[14] N. G. Paterakis, O. Erdinc, I.N. Pappi, A. G. Bakirtzis, J.P.S. Catalão, "Coordinated operation of a neighborhood of smart households comprising electric vehicles, energy storage and distributed generation", *IEEE Trans. on Smart Grid* , vol. 7, pp. 2736-2747, November. 2016.
[15] [Online]. Available: https://midcdmz.nrel.gov/
[16] [Online]. Available: http://www.liotech.ru/ensmallford